SAND2019-11944C

# Model Reduction of Wind Turbine Generator Models for Control Performance Evaluation

Felipe Wilches-Bernal
Sandia National Laboratories
Albuquerque, NM
fwilche@sandia.gov

Christoph Lackner
Grid Protection Alliance
Chattanooga, TN
clackner@gridprotectionalliance.org

Joe H. Chow
Rensselaer Polytechnic Institute
Troy, NY
chowj@rpi.edu

***Abstract*—Power system operations are fundamentally changed by the growing installation of wind generation systems. The undispatchable nature of wind turbine generators (WTGs) causes the operating conditions of power systems to be more volatile. At the same time, the converter-based interface of WTGs are capable, and are increasingly expected to, provide voltage and frequency regulation capabilities. Monitoring of power systems becomes critical under these anticipated conditions and high resolution data, such as synchrophasors, are crucial for this task. This paper presents an approximate low-order model of WTGs that can be readily estimated from available synchrophasor measurements. The identification of the parameters of the model can be used to approximate the control performance of WTGs and their contributions to frequency and voltage regulation.**

***Index Terms*—Model Reduction; System identification; Wind Turbine Generators; Wind Energy**

## I. Introduction

The power production energy mix is expected to accommodate increasing levels of converter-interfaced generation such as wind and solar systems [1]. In the span of 15 years, the cumulative wind capacity in the U.S. has grown from 6700 MW in 2004 to more than 97000 MW in 2019 [2]. Modern wind energy conversion systems are traditionally composed of multiple wind turbine generators (WTGs) which connect to the grid via power-electronics converters. The dynamics of the interaction between the WTGs and the grid are dominated by the converters and they are substantially different than those of synchronous generators (which make the bulk of the conventional generation). Hence, the regular operation of the power system is evolving as more and more converter-interfaced generation is connected to it.

Adequate operation of a power system requires controls aimed at keeping the frequency of the system constant and as close to the nominal value as possible. The power production at selected generating units is modulated to achieve this goal [3]. Additionally, voltages in the power system must be kept within a limited range. This problem is typically solved by controlling the reactive power available at the bus terminals of the system. Reactive power is controlled by both generating units and compensating devices such as capacitor banks and STATCOMs [3]. In power systems where wind generation plays a significant role in their power production, it is expected to contribute in providing frequency and voltage regulation [4]–[6].

Phasor measurement units (PMUs) provide *high* resolution data of power system signals. The data provided by these devices is time-tagged according to a common clock. The wide spread installation of PMUs has made their data available for different applications such as model validation, performance monitoring, and control [7]–[11]. Previous work has investigated how PMU data can be used to assess the control performance of conventional generators [12] and STATCOMS [13]. PMU data can be used to monitor and continuously update power system models particularly when the power system operating conditions are more volatile as is expected to happen with intermittent generation such as wind.

This work presents a reduced order model of a WTG. The model is derived from a linearization and a model reduction from a traditional and validated WTG model used in power system dynamic studies [14]. The proposed model is validated with simulated PMU data and is suited for assessing the control performance of WTGs. In particular, it can be used to evaluate the voltage and reactive power control as well as the power and frequency control performance of WTGs. The parameters defining the WTG model presented in this work can be identified from available PMU data.

This paper is organized as follows. Sections II and III introduce respectively the power system and complete WTG model used in this work. Section IV discusses the linearization of the WTG model. Section IV presents the reduced-order model and its validation in time and frequency domain. The conclusions and future work are presented in Section VI.

## II. Test Power System

The power system used in this work is presented in Fig. 1. It is an infinite-bus type of system that has three generating units in parallel. Two of these units are conventional generators: G1 and G2, and the third one is a WTG. The operating condition of the system is shown in Table I. The wind speed for the WTG is set a constant value of $14\ \mathrm{m/s}$ which is above the minimum wind speed required to produce the rated power.

Sandia National Laboratories is a multimission laboratory managed and operated by National Technology and Engineering Solutions of Sandia, LLC., a wholly owned subsidiary of Honeywell International, Inc., for the U.S. Department of Energy's National Nuclear Security Administration under contract DE-NA0003525.

This research was supported in part by the U.S. Department of Energy Transmission Reliability program.

This research was partly supported by the Engineering Research Center Program of the National Science Foundation and the Department of Energy under NSF Award Number EEC-1041877, NSF Award Number EEC-1550029, the CURENT Industry Partnership Program and NYSERDA under Award Number PON-3397.

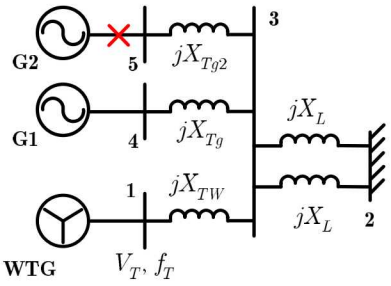


**Fig. 1:** Test system used in this work for WTG model validation.

**TABLE I:** Operating condition of the test system

| Device | P (MW) | Q (MVar) | V (pu) | $\theta$ (Deg.) |
|---|---|---|---|---|
| WTG | 350 | 129.43 | 1.05 | 26.7394 |
| $G_1$ | 250 | 85.07 | 1.05 | 27.76 |
| $G_2$ | 250 | 85.07 | 1.05 | 27.76 |

## III. WTG Dynamic Model

In order to determine the control performance of a single WTG, the first necessary step is to identify the independent response of the WTG *decoupled* from the response of the entire power network. Fig. 2 shows a WTG connected to the power system as well as its input and output signals. The active and reactive current injected by the WTG to the power system are determined by the voltage magnitude and frequency (note that the frequency is the derivative of the voltage angle) at the WTG point of interconnection (POI) [15]–[17]. Hence, the dynamics of the WTG can be described by

$$\dot{\mathbf{x}} = \mathbf{f}(\mathbf{x}, \mathbf{u}) \tag{1}$$

$$\begin{bmatrix} I_Q \\ I_P \end{bmatrix} = \mathbf{g}(\mathbf{x}, \mathbf{u}) \tag{2}$$

where,

$$\mathbf{u} = [V_T, f_T]^\top \tag{3}$$

are the inputs of the system, $V_T$ is the voltage magnitude, and $f_T$ is the frequency at the POI. Vector $\mathbf{x}$ represents the states of the WTG and $I_Q$ and $I_P$ respectively represent the WTG reactive and active current injections. The WTG under

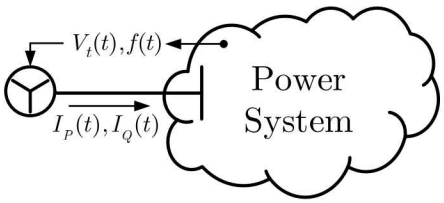


**Fig. 2:** WTG and its connection to the electric grid.

consideration in this work is a Type-3 WTG with independent active and reactive power control. Fig. 3 shows the active power control configuration and Fig. 4 shows the reactive power control. The pitch control, pitch compensation, and torque control blocks of the active power control are described by the following PI controllers

$$\text{Pitch Control: } G_{\text{cont}}(s) = K_{\text{pp}} + \frac{K_{\text{ip}}}{s} = 150 + \frac{25}{s} \tag{4}$$

$$\text{Pitch Comp.: } G_{\text{comp}}(s) = K_{\text{pc}} + \frac{K_{\text{ic}}}{s} = 3 + \frac{30}{s} \tag{5}$$

$$\text{Torque Control: } G_{\text{torq}}(s) = K_{\text{ptrq}} + \frac{K_{\text{itrq}}}{s} = 3 + \frac{0.6}{s} \tag{6}$$

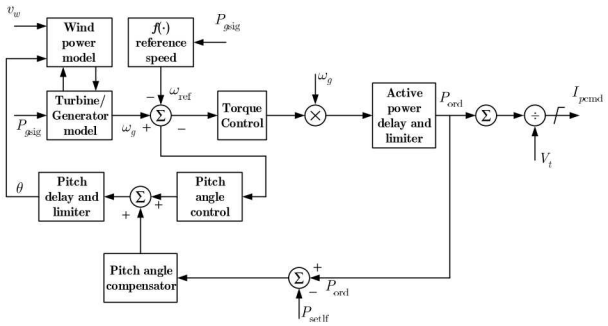


**Fig. 3:** Schematic of the active power control of the WTG.

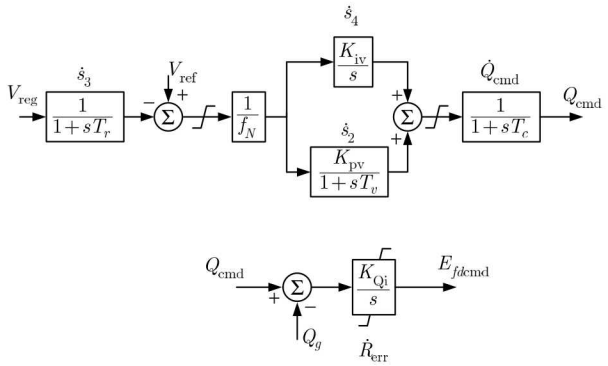


**Fig. 4:** Schematic of the reactive power control of the WTG.

The actual current injected by the WTG is

$$I_t = \left(I_p - j\frac{E_{fd}}{L_{pp}}\right)(\cos(\gamma) + j\sin(\gamma)) + j\frac{\tilde{V}_t}{L_{pp}} \tag{7}$$

$$= I_P + jI_Q \tag{8}$$

where $I_p$ and $E_{fd}$ correspond to the outputs of the active and reactive power controllers after they pass through a first order transfer function. $\tilde{V}_t$ is the voltage a the POI and $\gamma$ is a state representing the PLL action of the converter that is described by [16]

$$\dot{\gamma} = k_{pllp}[V_{\text{tim}}\cos(\gamma) - V_{\text{tre}}\sin(\gamma)]. \tag{9}$$

In (9), $\gamma$ is a state that follows the voltage angle at the POI which can be obtained from the knowledge of the frequency $f_T$ and the initial conditions of the system.

This work implemented the WTG model described in this section in a standalone manner where measurements of the inputs $V_T$ and $f_T$ can be used to obtain $I_Q$ and $I_P$ in open loop (without the need of a power network). The model was implemented in Simulink and was validated with simulated data from the system in Fig. 1.

## IV. Model Linearization

The WTG model in eqs. (1) and (2) is nonlinear and consist of 17 states. For evaluating the performance of the WTG controls a linearization of the system is convenient. Linearizing the WTG model will yield a matrix of transfer functions as follows

$$\begin{bmatrix}\Delta I_Q \\ \Delta I_P\end{bmatrix} = \begin{bmatrix}H_{VQ}(s) & H_{fQ}(s) \\ H_{VP}(s) & H_{fP}(s)\end{bmatrix}\begin{bmatrix}\Delta V_T \\ \Delta f_T\end{bmatrix} \tag{10}$$

where $H_{VQ}$ and $H_{fQ}$ are the transfer functions that relate the reactive current output of the WTG with $V_T$ and $f_T$, respectively. Similarly, transfer functions $H_{VP}$ and $H_{fP}$ relate $V_T$ and $f_T$ with the active current output of the WTG. Note that the linearization of the system in (10) is only valid for disturbances where the WTG is in a linear region, without hitting any limits. This is reflected by including a $\Delta$ symbol in front of the inputs and outputs of (10).

Simulations for different events of system in Fig. 1 are performed to obtain $V_T$ and $f_T$ measurement signals. These signals are then used to evaluate the performance of the linearized model in (10). Figs. 5a and 5b show, respectively, the reactive and active current outputs of the WTG linearized model and compares it against the simulated signal and the output of the standalone nonlinear model described in Section III. These results are for the loss of $G_2$ in Fig. 1 at $t = 1$s. The results in Fig. 5 show that the outputs of both the linearized model and the standalone nonlinear model completely align with the simulated/measured signal. These results show that for the event under consideration the linear version of the model is a valid representation of the WTG. Note that the initial conditions of the inputs were made zero.

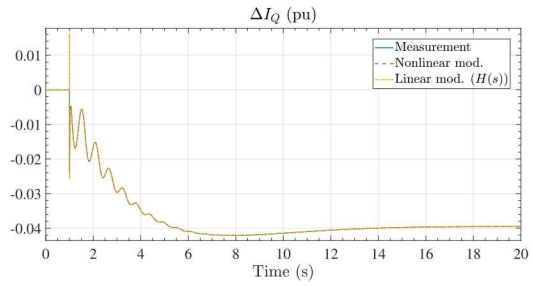


**(a)** WTG reactive current.

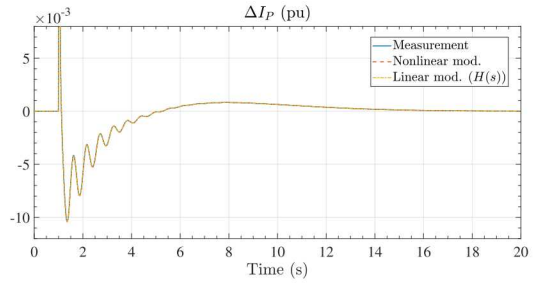


**(b)** WTG active current.

**Fig. 5:** Simulated output signals as well as the response of the linear and nonlinear system.

The linear model in (10) is a multiple input multiple output (MIMO) system with two inputs and two outputs. Each output is affected differently by each input. By rewriting (10) as

$$\Delta I_Q = H_{VQ}\Delta V_T + H_{fQ}\Delta f_T = \Delta I_{VQ} + \Delta I_{fQ} \tag{11}$$

$$\Delta I_P = H_{VP}\Delta V_T + H_{fP}\Delta f_T = \Delta I_{VP} + \Delta I_{fP}, \tag{12}$$

this work can explore the individual contribution of each input to the outputs of the system. Fig. 6a shows the individual responses of the WTG reactive power output $\Delta I_{VQ}$ and $\Delta I_{fQ}$ and compares them with the simulated signal. Fig. 6b shows the individual responses of the WTG active power output $\Delta I_{VP}$ and $\Delta I_{fP}$ and compares them with the simulated signal. Together, the results in Fig. 6 show that the contribution of the frequency input to the output is negligible for both the reactive and active current of the WTG. This means that the reactive current output can be approximated by $\Delta I_Q \approx H_{VQ}\Delta V_T$ and the active current by $\Delta I_P \approx H_{VP}\Delta V_T$. With this approximation the system can be thought as a multiple output single input (MISO) system. The results in time domain

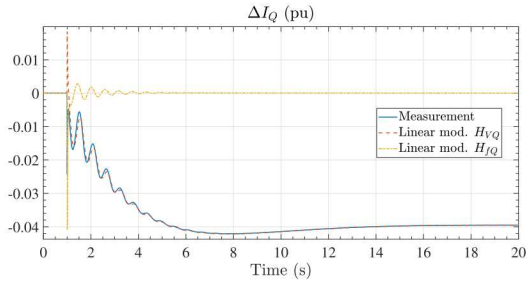


**(a)** WTG reactive current.

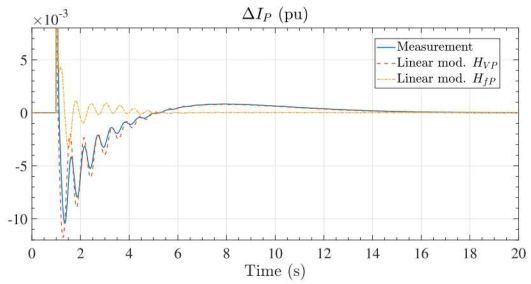


**(b)** WTG active current.

**Fig. 6:** Simulated output signals as well as the response of the individual transfer functions of the linear model.

shown in Fig. 6 are confirmed in the frequency domain. Fig. 7 shows the magnitude bode plot of $H_{VQ}$, $H_{fQ}$, $H_{VP}$, and $H_{fP}$ for a frequency interval from $10^{-2}$s to $10^{2}$s. These figures show that $|H_{VQ}| \gg |H_{fQ}|$ and $|H_{VP}| \gg |H_{fP}|$ for the plotted frequency range (which is wider than the interval of frequencies of interest).

Note that the WTG model under analysis does not have enabled controls for frequency regulation such as WindINER-TIA [17].

## V. Model Reduction

The linear representation of the WTG yields transfer functions of $17^{\text{th}}$ order. As shown in Section IV both the active and the reactive current outputs are mainly affected by only

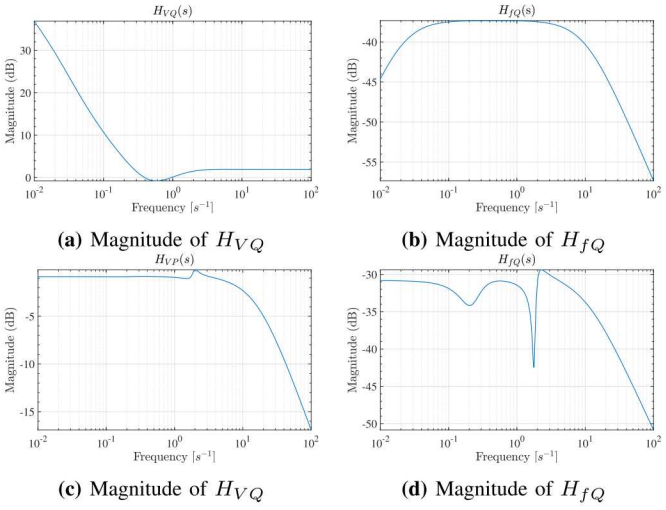


**(a)** Magnitude of $H_{VQ}$ **(b)** Magnitude of $H_{fQ}$

**(c)** Magnitude of $H_{VQ}$ **(d)** Magnitude of $H_{fQ}$

**Fig. 7:** Magnitude Bode plots of each of the transfer functions of $H(s)$.

one input: the WTG terminal voltage ($V_T$). Transfer functions of such a high order may be too complex to be determined from available system measurements. In this section the representation of the WTG was further simplified by a model order reduction of transfer functions: $H_{VQ}$ and $H_{VP}$.

This work uses Bode plots to help determine the frequency range of interest for the transfer functions to be reduced. The idea is to observe how the WTG transfer functions are affected with variations of the control parameters that determine the WTG active and reactive power controls. Nine parameters are used for this evaluation. Six from the active and three from the WTG reactive power control parameters; respectively: $k_{\mathrm{pc}}$, $k_{\mathrm{pp}}$, $k_{\mathrm{ptrq}}$, $k_{\mathrm{ic}}$, $k_{\mathrm{ip}}$, $k_{\mathrm{itrq}}$ and, $k_{\mathrm{iv}}$, $k_{\mathrm{pv}}$, $k_{\mathrm{Qi}}$. Fig. 8 shows Magnitude Bode plots of $H_{VQ}(s)$ for variations in the three reactive power control parameters. The results show that these parameters modify the transfer function only in the frequency range below 2 Hz. The variations of $H_{VQ}(s)$ with the six active power control parameters were also evaluated. They show $H_{VQ}(s)$ is unaffected by variation in those parameters and the figures are not shown here due to space constraints. Magnitude Bode plots are shown in Fig. 9c illustrating how $H_{VP}$ is affected by variations in some active power control parameters. The results in Fig. 9c shows that $H_{VP}$ is largely unaffected by variations on $k_{\mathrm{pc}}$, $k_{\mathrm{pp}}$, $k_{\mathrm{ptrq}}$. The results for the remaining three active power control parameters and the three reactive power control parameters are similar and show that variations in those parameters do not modify the transfer function.

The model reduction is performed for each transfer function individually. For transfer function $H_{VQ}(s)$ the model reduction was done according to the method proposed in [18] specifying a frequency range of interest from 0 to 2 Hz and an order of 2. A second order was selected because it was the minimum order for which the reduction yielded satisfactory results. The reduced order transfer function can be written as

$$\hat{H}_{VQ}(s) = \frac{-K_{VQ}(s+z_1)(s+z_2)}{s(s+p_1)} \tag{13}$$

where $z_1 = 0.326$, $z_2 = 2.473$, $p_1 = 0.132$ and $K_{VQ} = 0.777$. For transfer function $H_{VP}(s)$ it is noted that in the frequency range of interest the Bode Plot does remains constant. Observations in time domain also show that $I_P \propto V_T$. The reduced order model is then

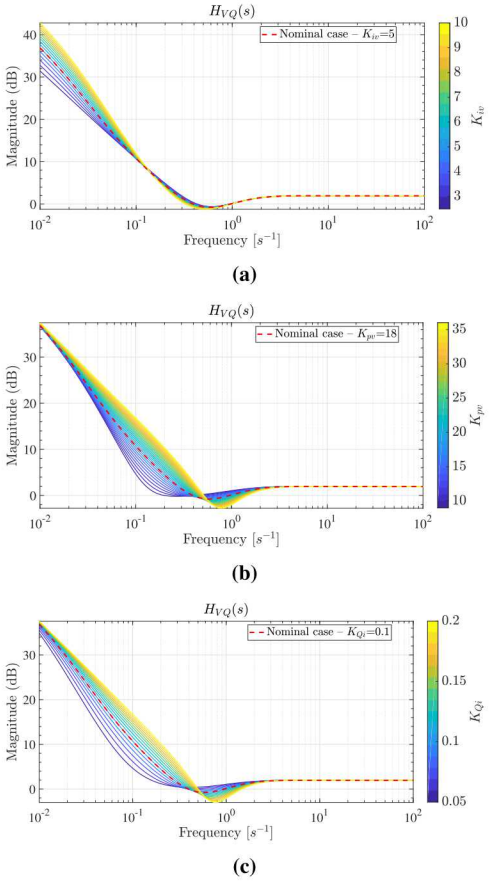


**(a)**

**(b)**

**(c)**

**Fig. 8:** Bode plot of $H_{VQ}$ as affected by variations in parameters: (a) $k_{\mathrm{iv}}$, (b) $k_{\mathrm{pv}}$, and (c) $k_{\mathrm{Qi}}$.

$$\hat{H}_{VP}(s) = -K_{VP} \tag{14}$$

where $K_{VP} = 0.907$. Note that in reality the reduced reduction yields a second order system with two poles and two zeros at the origin that cancel each other out.

Fig. 10a shows the output of the reduced order model of $\hat{H}_{VQ}(s)$ to the input $\Delta V_T$. This figure also shows the measured output $\Delta I_Q$. Fig. 10b shows the output of the reduced order model of $\hat{H}_{VQ}(s)$ to the input $\Delta V_T$ compared with the measured output $\Delta I_P$. The results in Fig. 10 show that the outputs generated by the reduced order model closely follow the measurement signal. They show that the reduced order model proposed in this work is a valid representation of the WTG for the type of disturbances considered in this work.

## VI. Conclusions and Future Work

This paper presents an approach to simplify a WTG model. The simplification is the product of a linearization followed by a model reduction. The initial linearized model is in itself obtained from a nonlinear standalone model. Like the full the model the simplified version has the reactive and active current

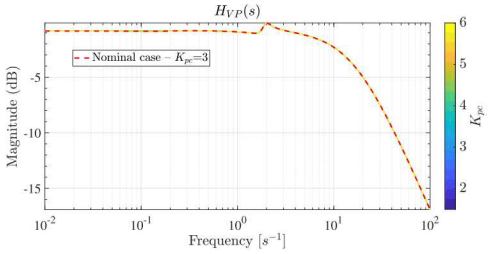


**(a)**

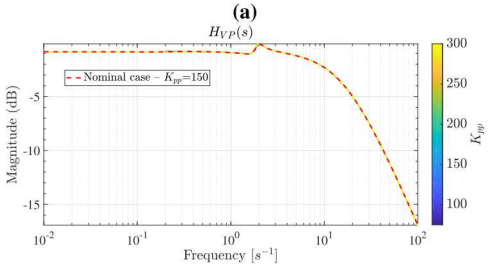


**(b)**

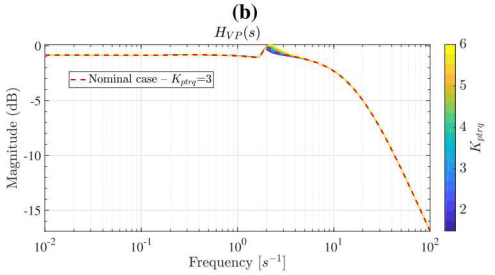


**(c)**

**Fig. 9:** Bode plot of $H_{VP}$ as affected by variations in parameters: (a) $k_{\mathrm{pc}}$, (b) $k_{\mathrm{pp}}$, (c) $k_{\mathrm{ptrq}}$.

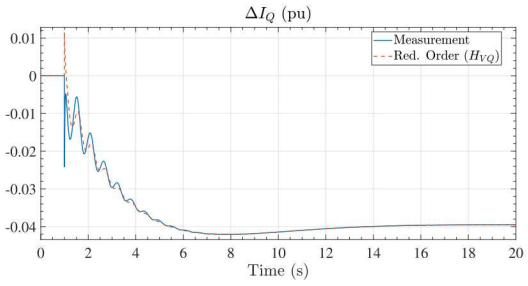


**(a)** WTG reactive current.

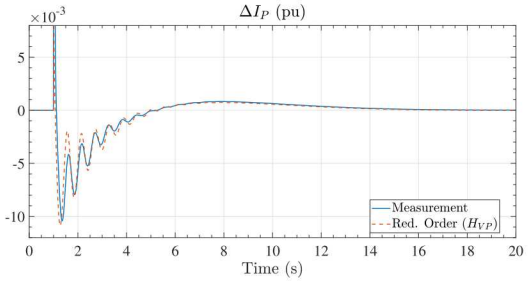


**(b)** WTG active current.

**Fig. 10:** Simulated output signals as well as the response of the reduced order system.

injections as outputs but unlike the full model the only relevant input is the voltage at the POI. The simplified model can be interpreted as a MISO system. The paper shows how the model reduction is performed and validated using time and frequency domain analysis in a test power system.

This model is presented because it will be used in future research to study the performance of the WTG control systems. The idea will be to use measured data, potentially from PMUs, to estimate the parameters that define the system proposed in this work. This idea has been successfully tested for both STATCOM [13] and conventional generators [12].

## REFERENCES


[1] T. Mai, D. Sandor, R. Wiser, and S. Thomas, "Renewable Electricity Futures Study: Executive Summary," National Renewable Energy Laboratory, Golden, CO, Tech. Rep. NREL/TP-6A20-52409-ES, 2023.

[2] American Wind Energy Association (AWEA). (2019) Wind facts at a glance. [Online]. Available: https://www.awea.org/wind-101/basics-of-wind-energy/wind-facts-at-a-glance

[3] P. Kundur, *Power System Stability and Control*. New York, NY: McGraw-Hill, 1994.

[4] N. Miller, R. Delmerico, K. Kuruvilla, and M. Shao, "Frequency responsive controls for wind plants in grids with wind high penetration," in *2012 IEEE Power and Energy Society General Meeting*. IEEE, 2012, pp. 1–7.

[5] N. Miller, J. MacDowell, G. Chmiel, R. Konopinski, D. Gautam, G. Laughter, and D. Hagen, "Coordinated voltage control for multiple wind plants in eastern wyoming: Analysis and field experience," in *2012 IEEE Power Electronics and Machines in Wind Applications*. IEEE, 2012, pp. 1–8.

[6] F. Wilches-Bernal, J. H. Chow, and J. J. Sanchez-Gasca, "A fundamental study of applying wind turbines for power system frequency control," *IEEE Transactions on Power Systems*, vol. 31, no. 2, pp. 1496–1505, 2015.

[7] Y. Li *et al*, "An innovative software tool suite for power plant model validation and parameter calibration using pmu measurements," in *Power & Energy Society General Meeting, 2017 IEEE*. IEEE, 2017, pp. 1–5.

[8] L. Sun, A. S. Meliopoulos, Y. Liu, and B. Xie, "Dynamic state estimation based synchronous generator model calibration using pmu data," in *Power & Energy Society General Meeting, 2017 IEEE*. IEEE, 2017, pp. 1–5.

[9] X. T. Jiang, J. H. Chow, and F. Wilches-Bernal, "A synchrophasor measurement based method for assessing damping torque contributions from power system stabilizers," in *2015 IEEE Eindhoven PowerTech*. IEEE, 2015, pp. 1–6.

[10] D. A. Schoenwald, B. J. Pierre, F. Wilches-Bernal, and D. J. Trudnowski, "Design and implementation of a wide-area damping controller using high voltage dc modulation and synchrophasor feedback," *IFAC-PapersOnLine*, vol. 50, no. 1, pp. 67–72, 2017.

[11] C. Lackner, J. H. Chow, and F. Wilches-Bernal, "Estimation of generator control system performance using synchrophasor data," in *XIV Symposium of Specialists in Electric Operational and Expansion Planning (SEPOPE)*, Recife, Brazil, 2018, pp. 1–12.

[12] C. Lackner, "Controls in power systems with renewable energy penetration," Ph.D. dissertation, Dept. Elect., Comput., and Syst. Eng., Rensselaer Polytechnic Inst., 2019.

[13] C. Lackner, J. H. Chow, and F. Wilches-Bernal, "Performance evaluation of STATCOM equipment using ambient and disturbance data,," in *the 13th PowerTech Conference*, Milan, Italy, 2019, pp. 1–6.

[14] M. Asmine *et al.*, "Model validation for wind turbine generator models," *IEEE Trans. Power Syst.*, vol. 26, no. 3, pp. 1769–1782, Aug. 2011.

[15] F. Wilches-Bernal, J. J. Sanchez-Gasca, and J. H. Chow, "Implementation of wind turbine generator models in the power system toolbox," in *Power and Energy Conf. at Illinois (PECI), 2014 IEEE*, Champaign, IL, 2014, pp. 1–5.

[16] *CIGRE Technical Brochure 318: Modeling and Dynamic Behavior of Wind Generation as it Relates to Power System Control and Dynamic Performance*, CIGRE, Paris, France, Aug. 2007.

[17] M. Shao, N. Miller, J. Sanchez-Gasca, and J. MacDowell, "Modeling of GE Wind Turbine-Generator for Grid Studies," General Electric International, Inc., Schenectady, NY, Tech. Rep. Version 4.6, Mar. 2013.

[18] A. Varga, "Balancing free square-root algorithm for computing singular perturbation approximations," in *Proceedings of the 30th IEEE Conference on Decision and Control*. Brighton, UK: IEEE, 1991, pp. 1062–1065.